Efficient MIMO PHY Abstraction with Imperfect CSI for Fast Simulations

Liu Cao, Lyutianyang Zhang, Sian Jin, and Sumit Roy, Fellow, IEEE

Abstract—This continues our prior work [1] on efficient PHY layer abstractions for scaling link simulations for complex scenarios, to include the important real-world impact of imperfect channel estimation. We extend the EESM-log-SGN abstraction by incorporating a model for effective SINR inclusive of channel estimation error, for multiple-input and multiple-output (MIMO) OFDM configurations, tailored towards IEEE 802.11ac/ax networks. The developed methods are then validated under different MIMO configurations for subsequent inclusion in ns-3 (www.nsnam.org) based cross-layer network performance evaluation.

Index Terms—PHY layer abstraction, EESM-log-SGN, Link-to-System (L2S), MMSE receiver.

I. Introduction

FULL PHY (link) simulations are necessary ingredients in quantifying network - Layer 2 MAC layer input/output - performance of modern IEEE 802.11 WLANs systems. However, executing a full PHY simulation that contains channel realization generations and transceiver signal processing within a network simulator is simply infeasible [1]. In addition, the growth in computational complexity of PHY simulation as links scale to larger channel bandwidths, high-dimension MIMO along with multi-user transmission, such in 802.11ax intended to support extremely high throughput (EHT) [2] is a manifest concern. To cope with such issues, PHY layer abstraction 1 is used to generate accurate link performance in a network simulator. The novel EESM-log-SGN PHY layer abstraction method ² achieves good accuracy in modeling the PHY layer, while its runtime is insensitive to growth in system dimensionality and is significantly lower compared to traditional PHY layer simulations.

Such efficient PHY layer abstractions for wideband frequency-selective fading channels rely on the suitable choice of link-to-system (L2S) mapping [3]–[8]. A L2S mapping function translates the post processing Signal-to-Interference-plus-Noise-Ratio (SINR) matrix into a single scalar metric called the *effective SINR* [9], that conveniently describes

Liu Cao, Lyutianyang Zhang, and Sumit Roy are with the Department of Electrical and Computer Engineering, University of Washington, Seattle, WA 98195 USA (e-mail: liucao@uw.edu; lyutiz@uw.edu; sroy@uw.edu). Sian Jin is with the Department of Electrical and Computer Engineering, Princeton University, Princeton, NJ 08544 USA (sj2434@princeton.edu) (Corresponding author: Liu Cao.)

¹The PHY layer abstraction is an equivalent packet error model used successful/unsuccessful MAC PDU reception based on the underlying PHY layer setup, for use in a network simulator such as ns-3.

²EESM-log-SGN PHY layer abstraction [1] bypasses the matrix calculation steps required by the traditional PHY layer abstraction methods, and directly models effective SINR by using a 4-parameter based log-SGN distribution.

packet-level performance in a network simulator by approximating the output with that from packet-level performance obtained from the full PHY simulations. Hence, representing the full transceiver processing chain by a single valued effective SINR is signficantly dependant on the choice of the L2S interface [8], [10].

As is well known, all systems requiring channel estimation implement this function at the receiver as part of receive decoding. For a variety of reasons, the estimated channel is inherently noisy in dense, overlapping network scenarios; the resultant imperfect channel state information (CSI) impacts the post processing SINR representing the PHY layer abstraction. To date, impact of such channel estimation errors as part of PHY layer abstraction has been ignored (i.e. estimation was assumed to be noise free) in prior art. Accordingly, the major contributions of this letter are summarized as follows.

• We improve the ideal CSI-based EESM-log-SGN PHY layer abstraction developed in [1] by considering the presence of imperfect CSI, intended for typical MIMO-OFDM Wi-Fi systems. An analytical model relating the channel estimation error and the effective SINR as a function of the channel estimation algorithm is used to develop the imperfect CSI-based EESM-log-SGN PHY layer abstraction ³ for use in network simulation.

II. SYSTEM ARCHITECTURE

A. MIMO Architecture

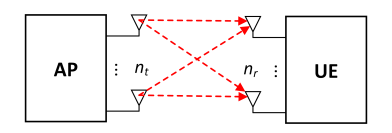


Fig. 1: DL OFDM SU-MIMO scenario.

As is shown in Fig. 1, we consider a scenario where an access point (AP) with n_t transmit antennas transmits downlink (DL) spatial streams to a single user (UE) with n_r receive antennas through Orthogonal Frequency Division Multiplexing (OFDM) in a single basic service set (BSS). The MIMO CSI acquisition schemes under such a scenario can be categorized into a) sounding reference signal (SRS)-based SU-MIMO, and b) precoding matrix indicator (PMI)-based SU-MIMO [11].

³All code used to generate the simulation results in this letter and the log-SGN parameters with imperfect CSI for different PHY configurations can be found at https://github.com/liucaouw/Code-for-EESM-log-SGN-PHY-abstraction-with-imperfect-CSI.

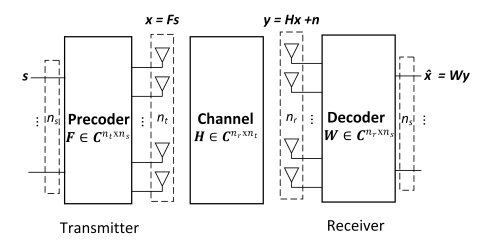


Fig. 2: MIMO architecture of typical Wi-Fi systems.

The multiple-input and multiple-output (MIMO) system model for typical DL Wi-Fi transmission is depicted in Fig. 2. We consider a frequency-selective channel, where the independent spatial flows are transmitted by using a set of subcarriers \mathcal{I}_{sc} . Suppose n_s modulated spatial streams are mapped into n_t transmit antennas on each subcarrier $i \in \mathcal{I}_{sc}$ by using a $n_t \times n_s$ precoding matrix $\mathbf{F}_i, i \in \mathcal{I}_{sc}$ [9]. A packet to be transmitted is then passed through a $n_r \times n_t$ frequency-domain channel matrix $\mathbf{H}_i, i \in \mathcal{I}_{sc}$ and arrives at the receiver with n_r receive antennas. Note that the channel matrix \mathbf{H}_i varies over the subcarrier index i due to the characteristics of the frequency-selective channel. The received signal on each subcarrier $i \in \mathcal{I}_{sc}$ can be thereby described as

$$\hat{\mathbf{x}}_i = \mathbf{W}_i \mathbf{H}_i \mathbf{F}_i \mathbf{s}_i + \mathbf{W}_i \mathbf{n}_i, \tag{1}$$

where $\mathbf{x}_i \in \mathbf{C}^{n_r}$, $\mathbf{W}_i \in \mathbf{C}^{n_s \times n_r}$, $\mathbf{H}_i \in \mathbf{C}^{n_r \times n_t}$, $\mathbf{F}_i \in \mathbf{C}^{n_t \times n_s}$, $\mathbf{s}_i \in \mathbf{C}^{n_s}$, and $\mathbf{n}_i \in \mathbf{C}^{n_r}$ denote the baseband signal at the receiver, decoding matrix, channel matrix, precoding matrix, basedband signal at the transmitter, repsectively. The additive noise vector at the receiving antenna conforms to zero mean circularly symmetric complex Gaussian (ZMCSCG) with variance σ^2 . In our work, we employ the minimum mean squared error (MMSE) detector which is expressed as [12]

$$\mathbf{W}_{i} = \left[(\mathbf{H}_{i} \mathbf{F}_{i})^{*} \mathbf{H}_{i} \mathbf{F}_{i} + \frac{\mathbf{I}}{SNR} \right]^{-1} (\mathbf{H}_{i} \mathbf{F}_{i})^{*}, \tag{2}$$

where $SNR = \frac{\mathbb{E}[(\mathbf{F}_i\mathbf{s}_i)^*(\mathbf{F}_i\mathbf{s}_i)]}{\mathbb{E}[\mathbf{n}_i^*\mathbf{n}_i]}$ is the ratio between the signal energy at each transmit antenna and the noise energy, and $\mathbb{E}[\bullet]$ denotes the expectation.

B. Link-to-system (L2S) mapping

At receiver's *i*-th subcarrier $i \in \mathcal{I}_{sc}$ and for stream $j \in \{1, 2, ..., n_s\}$, the post processing SINR $\Gamma_{i,j}$ is [4]

$$\Gamma_{i,j} = \frac{S_{i,j}}{I_{i,j}^s + N_{i,j}},\tag{3}$$

where $S_{i,j}$ is the signal power at the receiver, $I_{i,j}^s$ is the inter-stream interference, and $N_{i,j}$ is the post processing noise power. Specifically, according to [4], they can be expressed as $S_{i,j} = P_t \left| \left[\mathbf{W}_i \right]_j^* \mathbf{H}_i \left[\mathbf{F}_i \right]_j \right|^2$, $I_{i,j}^s = P_t | \left[\left[\mathbf{W}_i \right]_j^* \mathbf{H}_i \mathbf{F}_i \right] \right|^2 - S_{i,j}$, and $N_{i,j} = \sigma^2 | \left| \left[\mathbf{W}_i \right]_j^* \right|^2$, respectively, where P_t is the total signal power at receiver (over all subcarriers and streams), σ^2 is additive noise power on each subcarrier, $|| \bullet ||$ is the Euclidean norm of a vector, $[\bullet]_j$ is the j-th column of a matrix, and $[\bullet]^*$ is the conjugate transpose of a matrix. Then the post processing SINR matrix at receiver is defined as $\Gamma \triangleq (\Gamma_{i,j})_{i \in \mathcal{I}_{sc}, 1 \le j \le n_s}$ [1].

Each entry of the post processing SINR matrix, Γ , is then compressed by an L2S mapping function Φ into an effective SINR. It should be noted that the effective SINR produces the same instantaneous PER as the simulation which is executed under an AWGN-SISO channel. The effective SINR is given by [3]–[6]

$$\Gamma_{eff}^{sinr} = \alpha \Phi^{-1} \left(\frac{1}{n_{sc}} \frac{1}{n_{s}} \sum_{i \in \mathcal{I}_{sc}} \sum_{j=1}^{n_{s}} \Phi \left(\frac{\Gamma_{i,j}}{\beta} \right) \right), \tag{4}$$

where Φ^{-1} is the inverse L2S mapping function, \mathcal{I}_{sc} is the set of subcarriers, $n_{sc} \triangleq |\mathcal{I}_{sc}|$ is the number of subcarriers, n_s is the number of spatial streams, α and β are L2S mapping tuning parameters that depend on PHY layer configurations, e.g., channel type, OFDM MIMO setup, MCS and channel coding. The accuracy of the instantaneous PER prediction depends on the L2S mapping function Φ , such as Exponential Effective SINR Mapping (EESM) and Received Bit Information Rate (RBIR) mapping. In particular, EESM L2S mapping function is used in our work, where $\alpha = \beta$ and L2S mapping function $\Phi(x) = \exp(-x)$ [6]. As a result, Eq. (4) becomes

$$\Gamma_{eff}^{sinr} = -\beta \ln \left(\frac{1}{n_{sc}} \frac{1}{n_s} \sum_{i \in \mathcal{I}_{sc}} \sum_{j=1}^{n_s} \exp \left(-\frac{\Gamma_{i,j}}{\beta} \right) \right).$$
 (5)

III. SYSTEM MODEL

A. Simulation based PHY layer abstraction

The definition of the post processing SINR $\Gamma_{i,j}$ expressed in Eq. (3) holds if the channel is perfectly known at the receiver. However, in any real system, the channel matrix at any subcarrier $\mathbf{H}_i, \forall i \in \mathcal{I}_{sc}$ estimated by the receiver is inherently noisy, so we model the estimated channel matrix as

$$\hat{\mathbf{H}}_i = \mathbf{H}_i + \Delta \mathbf{H}_i, \tag{6}$$

where $\Delta \mathbf{H}_i$ denotes the estimation error matrix, assumed to be uncorrelated with \mathbf{H}_i , and each entry of \mathbf{H}_i follows ZMCSCG with variance σ_e^2 . The quality of channel estimation is captured by σ_e^2 , which depends on the channel estimation method used. We assume that each block (packet) undergoes an independent channel realization \mathbf{H}_i , as represented by a draw from $\Delta \mathbf{H}_i$ at the receiver.

As shown in Fig. 3, we first demonstrate the simulation flow chart that consists of the execution steps of the full PHY simulation 4 inclusive of model-based imperfect channel estimation. Based on the full PHY simulation, the packet-level performance under imperfect channel estimation is cataloged. Fig. 4 shows the average PER regarding the SNR under perfect and imperfect channel estimation through the full PHY simulation. One can observe that a small σ_e can cause large PER difference between different channel estimation qualities in each SNR points.

Subsequently, the post processing SINR matrix and the associated binary packet error state for each packet can be obtained after the full PHY simulation. The set {post processing SINR matrix Γ , binary packet error state} are then used to optimize the EESM tuning parameter β of the EESM mapping function [13]. The parameter β in Eq. (4) is then optimized to minimize

⁴The full PHY simulation is conducted via a reliable link simulator, e.g., MATLAB WLAN Toolbox, to produce calibrated L2S mapping tuning parameters.

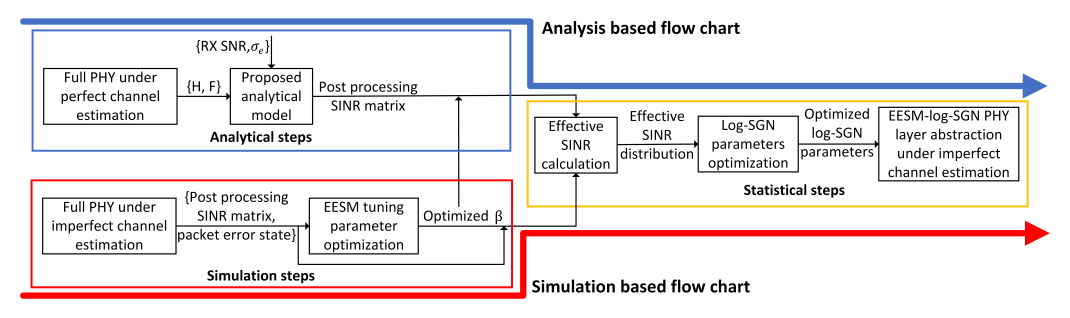


Fig. 3: Flow charts for implementing EESM-log-SGN PHY layer abstraction under imperfect channel estimation.

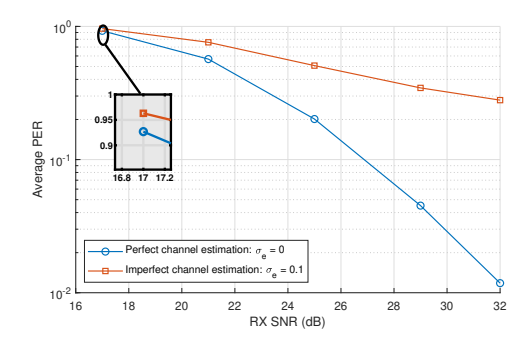


Fig. 4: Full PHY simulation: Average PER versus SNR under OFDM allocation with 242 subcarriers, 2 × 2 MIMO, IEEE TGax channel model-B, MCS5.

the mean square error (MSE) between the instantaneous PER-effective SINR curve for the simulated frequency-selective fading channel and the instantaneous PER-SNR curve under the AWGN-SISO channel. Then, in the initial stage of the statistical steps, an effective SINR distribution can be obtained through Eq. (4) with the optimized EESM parameter β and post processing SINR matrices of all packets.

Lemma 1. The effective SINR Γ_{eff}^{sinr} is independent of the channel estimation error parameter σ_e for MISO/SISO configuration.

Proof. Under MISO, \mathbf{W}_i is a scalar, as $n_r=1$ and only a single stream $n_s=1$ can be supported to the intended user. For the i-th subcarrier $i\in\mathcal{N}_{sc}$ and the only stream (indicated by $I_{i,1}^s=0$), the post processing SINR $\Gamma_{i,1}$ is expressed as $\Gamma_{i,1}=\frac{S_{i,1}}{N_{i,1}}$, where $S_{i,1}=P_t\,|[W_i]_1^*\mathbf{H}_i[\mathbf{F}_i]_1|^2=P_tW_i^2\,|\mathbf{H}_i[\mathbf{F}_i]_1|^2$, and $N_{i,1}=\sigma^2||[W_i]_1||^2=\sigma^2W_i^2$. Substituting $S_{i,1}$ and $N_{i,1}$ with the above, we get $\Gamma_{i,1}=\frac{P_t\,|\mathbf{H}_i[\mathbf{F}_i]_1|^2}{\sigma^2}$. Similarly, under SISO configuration, \mathbf{W}_i , \mathbf{H}_i and \mathbf{F}_i are all scalars, i.e., W_i , H_i and F_i , as $n_r=n_t=1$, and $n_s=1$. Hence $S_{i,1}=P_t\,|[W_i]_1^*H_iF_i|^2=P_tW_i^2H_i^2F_i^2$ and $N_{i,1}=\sigma^2||[W_i]_1||^2=\sigma^2W_i^2$. Then we get $\Gamma_{i,1}=\frac{P_tH_i^2F_i^2}{\sigma^2}$. From Eq. (5), the effective SINR under both configurations becomes $\Gamma_{eff}^{sinr}=-\beta\Phi^{-1}\left(\frac{1}{n_{sc}}\sum_{i\in\mathcal{I}_{sc}}\Phi\left(\frac{\Gamma_{i,1}}{\beta}\right)\right)$, which is independent of W_i and hence σ_e .

Remark 1. According to Lemma 1, the channel estimation error does not impact effective SINR distribution under MISO/SISO configuration. This does not hold under

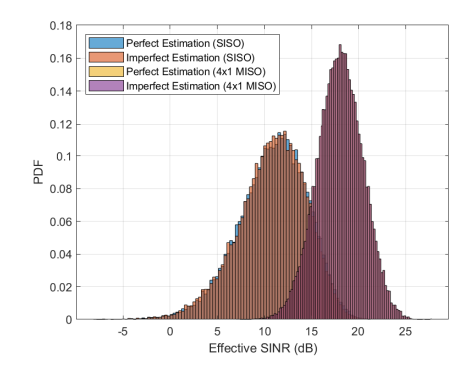


Fig. 5: Effective SINR distributions following simulation steps (SNR = 13dB).

MIMO/SIMO configuration as the post-processing SINR does depend on MMSE equalizer matrix \mathbf{W}_i .

As Fig.5 shows, the effective SNR distributions following the simulation steps overlap in the MISO/SISO case under the perfect and imperfect channel estimation. The obtained effective SINR distribution is then statistically fitted with the log-SGN distribution [1]

$$X \triangleq \ln(\Gamma_{eff}^{sinr}) \sim \text{SGN}(\hat{\mu}, \hat{\sigma}, \hat{\lambda}_1, \hat{\lambda}_2), \tag{7}$$

with the probability density function (PDF)

$$f_X(x; \hat{\mu}, \hat{\sigma}, \hat{\lambda}_1, \hat{\lambda}_2) = \frac{2}{\hat{\sigma}} \psi\left(\frac{x - \hat{\mu}}{\hat{\sigma}}\right) \Psi\left(\frac{\hat{\lambda}_1(x - \hat{\mu})}{\sqrt{\hat{\sigma}^2 + \hat{\lambda}_2(x - \hat{\mu})^2}}\right), \ x \in \mathbf{R},$$
(8)

where $\hat{\mu} \in \mathbf{R}$ is the location parameter, $\hat{\sigma} > 0$ is the scale parameter, $\hat{\lambda}_1 \in \mathbf{R}$ and $\hat{\lambda}_2 \geq 0$ are shape parameters, $\psi(x)$ is the standard normal PDF, and $\Psi(x)$ is the standard normal cumulative distribution function. The key information in the PHY layer in the existence of channel estimation error can be characterized by the log-SGN parameters based on the effective SINRs from full PHY simulation results under imperfect channel estimation.

B. Analysis based PHY layer abstraction

Fig. 3 shows a flow chart for the EESM-log-SGN PHY layer abstraction under imperfect channel estimation. The analytical method is a mix of original EESM-log-SGN model-based abstraction assuming perfect knowledge (i.e., channel matrix $\mathbf{H}_i, i \in \mathcal{I}_{sc}$ and precoding matrix $\mathbf{F}_i, i \in \mathcal{I}_{sc}$ of each

$$\mathbf{E}_{i} = \begin{pmatrix} \sigma_{e}^{2} \operatorname{tr}(\mathbf{K}_{i} \mathbf{F}_{i}^{*} \mathbf{H}_{i}^{*} \mathbf{H}_{i} \mathbf{F}_{i} \mathbf{F}_{i}^{*} \mathbf{H}_{i}^{*} \mathbf{H}_{i} \mathbf{F}_{i} \mathbf{K}_{i}^{*}) \mathbf{K}_{i} \mathbf{F}_{i}^{*} \mathbf{H}_{i}^{*} \mathbf{H}_{i} \mathbf{F}_{i} \mathbf{K}_{i}^{*} + \sigma_{e}^{2} \operatorname{tr}(\mathbf{H}_{i} \mathbf{F}_{i} \mathbf{K}_{i} \mathbf{F}_{i}^{*} \mathbf{H}_{i}^{*} \mathbf{H}_{i} \mathbf{F}_{i} \mathbf{K}_{i}^{*} \mathbf{F}_{i}^{*} \mathbf{H}_{i}^{*} \mathbf{H}_{i} \mathbf{F}_{i} \mathbf{K}_{i}^{*} \mathbf{K}_{i}^{*} + \sigma_{e}^{2} \operatorname{tr}(\mathbf{H}_{i} \mathbf{F}_{i} \mathbf{K}_{i}^{*} \mathbf{F}_{i}^{*} \mathbf{H}_{i}^{*} \mathbf{H}_{i} \mathbf{F}_{i} \mathbf{K}_{i}^{*} \mathbf{K}_{i}^{*} - \sigma_{e}^{2} \operatorname{tr}(\mathbf{H}_{i} \mathbf{F}_{i} \mathbf{F}_{i}^{*} \mathbf{H}_{i}^{*} \mathbf{H}_{i} \mathbf{F}_{i} \mathbf{K}_{i}^{*} \mathbf{F}_{i}^{*} \mathbf{H}_{i}^{*}) \mathbf{K}_{i} \mathbf{K}_{i}^{*} \\ + \sigma_{e}^{2} \operatorname{tr}(\mathbf{H}_{i} \mathbf{F}_{i} \mathbf{F}_{i}^{*} \mathbf{H}_{i}^{*}) \mathbf{K}_{i} \mathbf{K}_{i}^{*} + \operatorname{SNR}^{-1} \mathbf{W}_{i} \mathbf{W}_{i}^{*} \end{pmatrix}$$

$$(9)$$

$$\mathbf{N}_{i} = \begin{pmatrix} \operatorname{SNR}^{-1}\mathbf{W}_{i}\mathbf{W}_{i}^{*} + \operatorname{SNR}^{-1}\sigma_{e}^{2}\operatorname{tr}(\mathbf{K}_{i}\mathbf{F}_{i}^{*}\mathbf{H}_{i}^{*}\mathbf{H}_{i}\mathbf{F}_{i}\mathbf{K}_{i}^{*})\mathbf{K}_{i}\mathbf{F}_{i}^{*}\mathbf{H}_{i}^{*}\mathbf{H}_{i}\mathbf{F}_{i}\mathbf{K}_{i}^{*} \\ + \operatorname{SNR}^{-1}\sigma_{e}^{2}\operatorname{tr}(\mathbf{H}_{i}\mathbf{F}_{i}\mathbf{K}_{i}\mathbf{F}_{i}^{*}\mathbf{H}_{i}^{*}\mathbf{H}_{i}\mathbf{F}_{i}\mathbf{K}_{i}^{*}\mathbf{F}_{i}^{*}\mathbf{H}_{i}^{*})\mathbf{K}_{i}\mathbf{K}_{i}^{*} - \operatorname{SNR}^{-1}\sigma_{e}^{2}\operatorname{tr}(\mathbf{H}_{i}\mathbf{F}_{i}\mathbf{K}_{i}\mathbf{F}_{i}^{*}\mathbf{H}_{i}^{*})\mathbf{K}_{i}\mathbf{K}_{i}^{*} - \operatorname{SNR}^{-1}\sigma_{e}^{2}\operatorname{tr}(\mathbf{H}_{i}\mathbf{F}_{i}\mathbf{K}_{i}\mathbf{F}_{i}^{*}\mathbf{H}_{i}^{*})\mathbf{K}_{i}\mathbf{K}_{i}^{*} + \operatorname{SNR}^{-1}\sigma_{e}^{2}N_{r}\mathbf{K}_{i}\mathbf{K}_{i}^{*} \end{pmatrix}$$

$$(10)$$

packet) combined with model based representation of MIMO channel estimation error developed earlier. Then a complete model is developed that relates the channel estimation error and the effective SINR for the imperfect CSI case, which is a function of the SNR, σ_e^2 and other system parameters. After the analytical steps, the analytical post processing SINRs under imperfect channel estimation are obtained. The above completes development of the steps comprising EESM-log-SGN PHY abstraction considering imperfect CSI, based on the analytical model obtained for effective SINR distribution. Note that given a fixed SNR, different packets are now characterized by the statistics of $\hat{\Gamma}_{eff}^{sinr}$ resulting from the block fading channels and MMSE channel estimation. In the rest of this section, we present the analytical model for effective SINR for MMSE detector with channel estimation error.

Following Eq. (2), the receiver can use the imperfect estimated channel to calculate the MMSE detector as follows,

$$\hat{\mathbf{W}}_{i} = [(\mathbf{H}_{i}\mathbf{F}_{i} + \Delta\mathbf{H}_{i}\mathbf{F}_{i})^{*}(\mathbf{H}_{i}\mathbf{F}_{i} + \Delta\mathbf{H}_{i}\mathbf{F}_{i}) + \frac{\mathbf{I}}{SNR}]^{-1} \bullet$$

$$(\mathbf{H}_{i}\mathbf{F}_{i} + \Delta\mathbf{H}_{i}\mathbf{F}_{i})^{*}$$

$$= [\mathbf{F}_{i}^{*}\mathbf{H}_{i}^{*}\mathbf{H}_{i}\mathbf{F}_{i} + \frac{\mathbf{I}}{SNR} + \mathbf{F}_{i}^{*}\mathbf{H}_{i}^{*}\Delta\mathbf{H}_{i}\mathbf{F}_{i}$$

$$+ \mathbf{F}_{i}^{*}\Delta\mathbf{H}_{i}^{*}\mathbf{H}_{i}\mathbf{F}_{i}]^{-1} \bullet \mathbf{F}_{i}^{*}(\mathbf{H}_{i} + \Delta\mathbf{H}_{i})^{*},$$
(11)

where we ignore the term $\mathbf{F}_i^*\Delta\mathbf{H}_i^*\Delta\mathbf{H}_i\mathbf{F}_i$ since it is much less significant than the channel estimation error $\Delta\mathbf{H}_i$ when σ_e^2 is small. With imperfect channel estimation, $\Delta\mathbf{H}_i$, the imperfect MMSE solution can also be written as $\hat{\mathbf{W}}_i = \mathbf{W}_i + \Delta\mathbf{W}_i$. Thus the MMSE estimate of the signal vector becomes

$$\hat{\mathbf{x}}_i = \hat{\mathbf{W}}_i \mathbf{y}_i = \mathbf{W}_i \mathbf{H}_i \mathbf{x}_i + \Delta \mathbf{W}_i \mathbf{H}_i \mathbf{x}_i + \mathbf{W}_i \mathbf{n}_i + \Delta \mathbf{W}_i \mathbf{n}_i, \quad (12)$$

where $\mathbf{x} = \mathbf{F}\mathbf{s}$ represents the precoded base-band data streams, and \mathbf{s} is the original signal. Denote $\mathbf{K}_i = (\mathbf{H}_i^* \mathbf{F}_i^* \mathbf{F}_i \mathbf{H}_i + \frac{\mathbf{I}}{\text{SNR}})^{-1}$, then based on $(\mathbf{P} + \epsilon^2 \mathbf{Q})^{-1} \approx \mathbf{P}^{-1} - \epsilon^2 \mathbf{P}^{-1} \mathbf{Q} \mathbf{P}^{-1}$ given small ϵ^2 we have the following,

$$\hat{\mathbf{W}}_{i} = (\mathbf{K}_{i} - \mathbf{K}_{i}(\mathbf{F}_{i}^{*}\mathbf{H}_{i}^{*}\Delta\mathbf{H}_{i}\mathbf{F}_{i} + \mathbf{F}_{i}^{*}\Delta\mathbf{H}_{i}^{*}\mathbf{H}_{i}\mathbf{F}_{i})\mathbf{K}_{i})\bullet (\mathbf{H}_{i}\mathbf{F}_{i} + \Delta\mathbf{H}_{i}\mathbf{F}_{i})^{*},$$
(13)

where $\triangle \mathbf{W}_i$ can be approximated as $-\mathbf{K}_i(\mathbf{F}_i^*\mathbf{H}_i^*\Delta\mathbf{H}_i\mathbf{F}_i + \mathbf{F}_i^*\Delta\mathbf{H}_i^*\mathbf{H}_i\mathbf{F}_i)\mathbf{K}_i\mathbf{F}_i^*\mathbf{H}_i^* + \mathbf{K}_i\mathbf{F}_i^*\Delta\mathbf{H}_i^*$.

$$\mathbb{E}[(\hat{\mathbf{W}}_{i}\mathbf{H}_{i}\mathbf{F}_{i})(\hat{\mathbf{W}}_{i}\mathbf{H}_{i}\mathbf{F}_{i})^{*}]$$

$$=\mathbb{E}[((\mathbf{W}_{i}+\Delta\mathbf{W}_{i})\mathbf{H}_{i}\mathbf{F}_{i})((\mathbf{W}_{i}+\Delta\mathbf{W}_{i})\mathbf{H}_{i}\mathbf{F}_{i})^{*}]$$

$$=\mathbb{E}[\mathbf{W}_{i}\mathbf{H}_{i}\mathbf{F}_{i}\mathbf{F}_{i}^{*}\mathbf{H}_{i}^{*}\mathbf{W}_{i}^{*}]+\mathbb{E}[\Delta\mathbf{W}_{i}\mathbf{H}_{i}\mathbf{F}_{i}\mathbf{F}_{i}^{*}\mathbf{H}_{i}^{*}\Delta\mathbf{W}_{i}^{*}]$$

$$=\mathbf{W}_{i}\mathbf{H}_{i}\mathbf{F}_{i}\mathbf{F}_{i}^{*}\mathbf{H}_{i}^{*}\mathbf{W}_{i}^{*}+\mathbf{E}_{i}$$
(14)

where \mathbf{E}_i is obtained with property $\mathbb{E}[\Delta \mathbf{H} \mathbf{A} \Delta \mathbf{H}] = \mathbb{E}[\Delta \mathbf{H}^* \mathbf{A} \Delta \mathbf{H}^*] = 0$ and $\mathbb{E}[\Delta \mathbf{H} \mathbf{A} \Delta \mathbf{H}^*] = \sigma_e^2 \mathrm{tr}(\mathbf{A}) \mathbf{I}$ in Eq. (9). The corresponding SINR is expressed as

$$\hat{\Gamma}_{i,j} = \frac{|(\mathbf{W}_i \mathbf{H}_i \mathbf{F}_i \mathbf{F}_i^* \mathbf{H}_i^* \mathbf{W}_i^* + \mathbf{E}_i)_{j,j}|^2}{\sum_{l \neq j} |(\mathbf{W}_i \mathbf{H}_i \mathbf{F}_i \mathbf{F}_i^* \mathbf{H}_i^* \mathbf{W}_i^* + \mathbf{E}_i)_{j,l}|^2 + [\mathbf{N}_i]_{j,j}},$$
 (15)

TABLE I: PHY layer simulation setup.

Communication system	IEEE 802.11ax
Link simulator	MATLAB WLAN Toolbox R2021b
Number of packets/simulation	20000
Channel type	IEEE TGax channel model-B [14]
Channel for each packet	i.i.d.
Speed of the scatter/user	0.089km/h
Channel coding	LDPC
Payload length	1000 bytes
MCS	5
Bandwidth	20 MHz (242 subcarriers in total)
Channel estimation error	ZMCSCG
MIMO/MU-MIMO PHY	SVD/ZF precoding, MMSE decoding
CPU	Intel Core i7 CPU at 2.60GHz

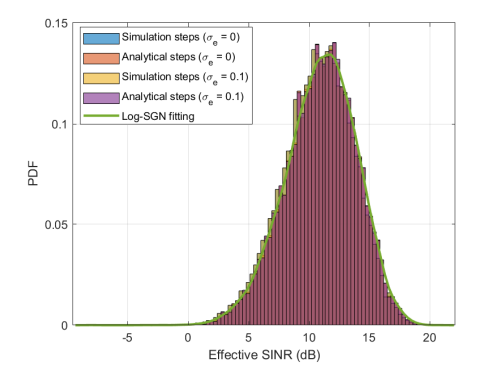


Fig. 6: Effective SINR distribution: Perfect/Imperfect channel estimation under 2×1 MISO (SNR = 9dB) configuration.

where

$$\mathbf{N}_{i} = \mathbb{E}[\mathbf{W}_{i}\mathbf{n}_{i}\mathbf{n}_{i}^{*}\mathbf{W}_{i}^{*}] + \mathbb{E}[\mathbf{W}_{i}\mathbf{n}_{i}\mathbf{n}_{i}^{*}\Delta\mathbf{W}_{i}^{*}] + \mathbb{E}[\Delta\mathbf{W}_{i}\mathbf{n}_{i}\mathbf{n}_{i}^{*}\mathbf{W}_{i}^{*}] + \mathbb{E}[\Delta\mathbf{W}_{i}\mathbf{n}_{i}\mathbf{n}_{i}\Delta\mathbf{W}_{i}^{*}]$$

$$+ \mathbb{E}[\Delta\mathbf{W}_{i}\mathbf{n}_{i}\mathbf{n}_{i}\Delta\mathbf{W}_{i}^{*}]$$
(16)

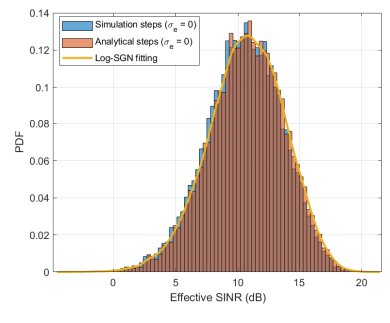
represents the expected noise power that can be further expressed in Eq. (10), using the property that $\mathbb{E}[\Delta \mathbf{W}] = 0$, $\mathbb{E}[\Delta \mathbf{H} \mathbf{A} \Delta \mathbf{H}] = \mathbb{E}[\Delta \mathbf{H}^* \mathbf{A} \Delta \mathbf{H}^*] = 0$ and $\mathbb{E}[\Delta \mathbf{H} \mathbf{A} \Delta \mathbf{H}^*] = \sigma_e^2 \mathrm{tr}(\mathbf{A})\mathbf{I}$. Hence, the effective SINR under imperfect channel estimation is finally given by

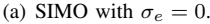
$$\hat{\Gamma}_{eff}^{sinr} = -\hat{\beta} \ln \left(\frac{1}{n_{sc}} \frac{1}{n_{s}} \sum_{i \in \mathcal{I}_{sc}} \sum_{j=1}^{n_{s}} \exp \left(-\frac{\hat{\Gamma}_{i,j}}{\hat{\beta}} \right) \right), \tag{17}$$

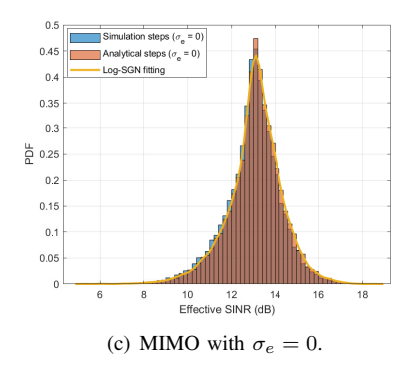
where $\hat{\Gamma}_{i,j}$ is expressed in Eq. (15), and $\hat{\beta}$ is obtained from the simulation steps. Since $\hat{X} \triangleq \ln(\hat{\Gamma}_{eff}^{sinr})$ is well-approximated by log-SGN distribution as per Eq. (7), we now have a full statistical characterization of the effective SINR imperfect channel estimation.

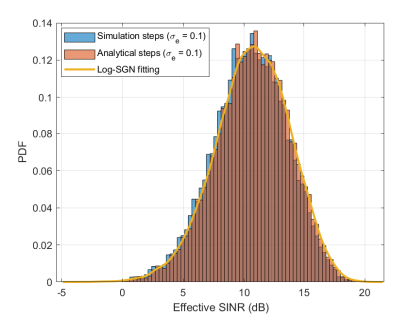
IV. VALIDATION

This section explores the effective SINR distribution following the analysis based flow chart for PHY system configurations described by Table I. First, we validate the MISO

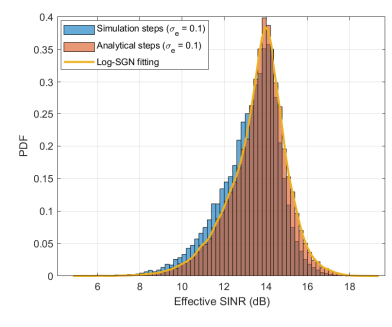








(b) SIMO with $\sigma_e = 0.1$.



(d) MIMO with $\sigma_e = 0.1$.

Fig. 7: Effective SINR distribution: Perfect/Imperfect channel estimation under 1×2 SIMO (SNR = 9dB)/2 $\times 2$ MIMO (SNR = 17dB) configuration.

configuration whose results are shown in Fig. 6; the effective SINR distribution obtained analytically in Lemma 1 matches with the empirical p.d.f obtained from simulation where we used a fitting method to extract the log-SGN parameters in Eq. (7). As the log-SGN fitting curve matches the analytical SINR distribution, the obtained log-SGN parameters accurately describe the end-to-end PHY layer abstraction.

Next, we investigate the developed method for single-input and multiple-output (SIMO) and MIMO configurations. As Fig. 7 shows, the analytical effective SINR distribution fits the corresponding empirical one obtained from the simulation for both cases, with the appropriate parameter fits. Note that compared with the SIMO case (Fig. 7(a) and (b)), the shapes of effective SINR distribution under MIMO (Fig. 7(c) and (d)) are more divergent with the same channel estimation quality. This is because the channel estimation error for MIMO impacts the post processing SINR more significantly than that under SIMO configuration. In summary, the log-SGN distribution with suitable parameters can accurately describe the effective SINR under all configurations considering imperfect CSI.

V. CONCLUSION

In this letter, we improved the EESM-log-SGN PHY layer abstraction to include imperfect CSI for DL OFDM SU-MIMO network. The code provided can generate the log-SGN parameters for DL single BSS network simulation scenarios. Future work will explore extensions for network scaling, i.e. multi-BSS OFDM/OFDMA MIMO networks with imperfect CSI.

REFERENCES

- S. Jin, S. Roy, and T. R. Henderson, "Efficient PHY layer abstraction for fast simulations in complex system environments," *IEEE Transactions* on *Communications*, vol. 69, no. 8, pp. 5649–5660, 2021.
- [2] S. Roy, T. Henderson, H. Yin, L. Cao, S. Jin, and L. Lanante, "Ns-3 WiFi Working Group: Update on 802.11ax & .be models," University of Washington, Tech. Rep. IEEE 802.11-22/1072r2, July 2022.
- [3] R. P. F. Hoefel and O. Bejarano, "On application of PHY layer abstraction techniques for system level simulation and adaptive modulation in ieee 802.11 ac/ax systems," *Journal of Communication and Information Systems*, vol. 31, no. 1, 2016.
- [4] IEEE TGax Group, "IEEE p802.11 wireless lans: 11ax evaluation methodology," 2016.
- methodology," 2016.
 [5] Mathworks, "Physical layer abstraction for system-level simulation," 2021
- [6] IEEE TGax Group, "Phy abstraction method comparison," in IEEE 802.11-14/0647r2, 2014.
- [7] K. Brueninghaus et al., "Link performance models for system level simulations of broadband radio access systems," in 2005 IEEE 16th International Symposium on Personal, Indoor and Mobile Radio Communications, vol. 4. IEEE, 2005, pp. 2306–2311.
- [8] L. Wan, S. Tsai, and M. Almgren, "A fading-insensitive performance metric for a unified link quality model," in *IEEE Wireless Communica*tions and Networking Conference, 2006. WCNC 2006., vol. 4. IEEE, 2006, pp. 2110–2114.
- [9] R. W. Heath Jr. and A. Lozano, Foundations of MIMO Communication. Cambridge University Press, 2018.
- [10] Lei Wan, Shiauhe Tsai, and M. Almgren, "A fading-insensitive performance metric for a unified link quality model," in *IEEE WCNC*, vol. 4, 2006, pp. 2110–2114.
- [11] Samsung, "Technical White Paper Massive MIMO for New Radio," Samsung, Tech. Rep., Dec 2020.
- [12] E. Eraslan, B. Daneshrad, and C.-Y. Lou, "Performance indicator for MIMO MMSE receivers in the presence of channel estimation error," *IEEE Wireless Communications Letters*, vol. 2, no. 2, pp. 211–214, 2013.
- [13] A. M. Cipriano, R. Visoz, and T. Salzer, "Calibration issues of PHY layer abstractions for wireless broadband systems," in 2008 IEEE 68th Vehicular Technology Conference. IEEE, 2008, pp. 1–5.
- [14] IEEE TGax Group, "Ieee 802.11ax channel model document," 2014.